https://doi.org/10.5194/egusphere-2026-4306
Preprint. Discussion started: 21 August 2026

Quantifying the impact of Light Absorbing Impurities on snow properties and melting using mini-lysimeters in the Central Pyrenees

Javier Bandrés[1], Jorge Pey[1], Esteban Alonso-González[1], Pablo Domínguez-Aguilar[1], Jesús Revuelto[1], Eñaut Izagirre[1, 2], Francisco Rojas-Heredia[1], Eric Allan Sproles[3], and Juan Ignacio López-Moreno[1]

1 Instituto Pirenaico de Ecología (IPE-CSIC), Zaragoza, 50059, Spain
2 Department of Geography, Universitat de Barcelona, Barcelona, 08001, Spain
3 Department of Earth Sciences and Geospatial Core Facility, Montana State University, Bozeman, MT, USA

Correspondence to: Javier Bandrés (jbandres@ipe.csic.es)

Abstract

The Pyrenees are experiencing an increasing frequency of atmospheric conditions favorable to African dust transport, while black carbon (BC) deposition is expected to decline in the coming decades. These two dominant light-absorbing impurities (LAIs) significantly alter snowpack properties by reducing snow surface albedo, accelerating melt, and disrupting mountain hydrology by modifying the surface energy balance. While the role of LAIs in enhancing snow metamorphism and melt is well recognized, quantifying their precise impact remains challenging due to the irregularity of deposition events, variability in impurity type and concentration, and the snowpack heterogeneity.

To better quantify and constrain the physical impacts of LAIs on snowpack, we implemented controlled field experiments using custom mini-lysimeters filled with natural snow, artificially doped with realistic concentrations of mineral dust (2, 5, 10 g/m^2) and BC (0.1, 0.2 g/m^2) and exposed to environmental conditions and sunlight for 3-4 hours in each set of experiments. Results revealed a systematic broadband albedo reduction of 0.2-0.3, accompanied by a marked decline in specific surface area (from ~10 to <4 m^2/kg in dust-treated samples). Seasonal mean liquid water content increased from 3.1% in clean snow to 6.2% (2 g/m^2 dust) and up to 10.1% (10 g/m^2 dust), with BC showing intermediate responses. However, the most striking effect was observed in meltwater production: even the lowest dust load frequently doubled melt rates relative to controls, and in several cases induced melt when control snow remained stable. Mineral dust outperformed BC in enhancing melt under comparable radiative conditions.

Overall, this study provides a simple and robust experimental framework for linking particle concentration to measurable changes in snow metamorphism and melt. Our results suggest that realistic concentrations of mineral dust, such as those frequently observed in the Pyrenees due to African dust deposition, can shorten snow duration and potentially reinforce the effects of ongoing climate warming.

https://doi.org/10.5194/egusphere-2026-4306
Preprint. Discussion started: 21 August 2026

1. Introduction

Seasonal snow plays a critical role in Earth's energy budget and water cycle (Flanner et al., 2011). In mountain catchments, particularly in Mediterranean mountain regions, accumulated snow acts as a major regulator of water availability by sustaining meltwater supply through spring and summer, when demands from both ecosystems and human activities are highest (Fayad et al., 2017; Musselman et al., 2021). However, Europe is currently the fastest-warming continent, with temperatures increasing at nearly twice the global average since the 1980s (Copernicus Climate Service, 2023). This warming is driving a marked decline in snow cover across European temperate mountains, particularly at mid-elevations (Bayle et al., 2025), leading to shorter snow seasons characterized by fewer days of snow cover and snowlines moving up in elevation, trends that are both expected to intensify in the coming decades (Vaughan et al., 2013; Beniston et al., 2018). In addition, winter snowmelt appears to be more sensitive to temperature increases than to precipitation changes (Gobiet et al., 2014; Beniston & Stoffel, 2014; López-Moreno et al., 2017; Pendergrass et al., 2017; Switanek et al., 2024), and they exhibit strong spatial and temporal variability across mountain regions (Laternser & Schneebeli, 2003; Valt & Cianfarra, 2010; Marcolini, 2017).

In addition to climatic factors, the role of light-absorbing impurities (LAIs) on the physical properties of snow-covered surfaces is increasingly relevant. The effects of LAIs on snow can be assessed through complementary physical and optical properties. Broadband albedo controls the fraction of incoming solar radiation reflected by the snowpack, whereas spectral albedo is particularly sensitive to the presence of LAIs. Specific surface area (SSA) characterizes snow metamorphism, while liquid water content (LWC) reflects the progression of snowmelt. It is well known that these particles, such as mineral dust and black carbon (BC), cause positive radiative forcing by absorbing radiation, reducing albedo in the visible and near infrared domains (300-2500 nm), and accelerating surface snowmelt (Hansen & Nazarenko, 2003; Painter et al., 2012; Skiles et al., 2018). LAIs indeed accelerate the coarsening of the snow microstructure, enhancing solar energy absorption and intensifying the intrinsic snow albedo feedback (Dumont et al., 2014; Skiles & Painter, 2018; 2019). Furthermore, LAIs are partially retained at the snow surface during melt, progressively amplifying the reduction in albedo over time (Sterle et al., 2013; Tuzet et al., 2020). Consequently, their impact on snow is influenced by meteorological conditions, leading to complex interactions between LAIs and the climatic drivers that govern snow cover evolution (Flanner et al., 2011). These interactions can affect runoff timing, water availability and mountain hydrology (Skiles et al., 2018; Revuelto et al., 2022).

Various types of LAIs can be found in alpine snowpacks, including mineral dust (Pey et al., 2020), black and organic carbon (Hadley & Kirchstetter, 2012), volcanic ash (Liu et al., 2014; Arnalds et al., 2016), snow algae (Remias et al., 2010), and microplastics (Marín-Beltrán et al., 2026). Their impact on snow has been investigated for more than a century, beginning with the work of Jones (1913) in the United States. More recently,

https://doi.org/10.5194/egusphere-2026-4306
Preprint. Discussion started: 21 August 2026

studies in the western United States using aerial, satellite, and ground-based observations (Painter et al., 2012, 2013b, 2018; Skiles et al., 2012; Reynolds et al., 2014), as well as investigations in Iceland (Dagsson-Waldhauserova et al., 2015; Wittmann et al., 2017), the Himalayas (Gautam et al., 2013), Greenland and Norway (Doherty et al., 2010), the Pyrenees (Pey et al., 2020; Bandrés et al., 2026), and the European Alps (Di Mauro et al., 2015; Dumont et al., 2017; Tuzet et al., 2017; Greilinger et al., 2018; Réveillet et al., 2020) have demonstrated the significant influence of LAIs, particularly mineral dust, on snow optical properties, energy balance, and snowpack evolution. In the Arctic, research has also highlighted the growing importance of natural aerosols, including mineral dust and biogenic emissions, in climate-driven changes (Schmale et al., 2021).

Europe is predominantly influenced by African dust, which accounts for around 50-70% of the continent's annual dust load (Ginoux et al., 2001). Aerosol deposition occurs predominantly through wet processes and is uneven, especially during African dust events. In southern European mountain regions such as the Pyrenees, mineral dust and BC are commonly found as LAIs on snow surfaces, making them key drivers of snowpack darkening and melt acceleration (Bandrés et al., 2026).

North Africa is one of the major global source regions of atmospheric mineral dust, contributing approximately 60% of total dust emissions worldwide (Shao et al., 2011). Once emitted, mineral dust can be transported over thousands of kilometers and episodically reaches the Mediterranean basin and southern Europe, including the Pyrenees (Barkan et al., 2004, 2005; Klein et al., 2010). In the Pyrenees, North African air masses are observed on approximately 15% of days each year (Pey et al., 2013; Bandrés et al., 2026), providing recurrent opportunities for mineral dust deposition onto the seasonal snowpack. The transported material is predominantly mineral and contains elements such as Fe, Ca, Si, K, Mg, and P.

Similarly, BC is a highly efficient light-absorbing aerosol (Flanner et al., 2007; Skiles et al.,2018) produced by the incomplete combustion of fossil fuels, biomass, and biofuels. Primary sources include emissions from diesel engines, coal burning, forest and agricultural fires, and residential wood burning (Bond et al., 2004; Bond et al., 2013). Once emitted, BC particles can be transported over long distances before being deposited via precipitation or dry deposition, and they are a key contributor to climate forcing, absorbing substantial solar radiation (IPCC, 2007). Historically, BC deposition increased across central Europe from 1850 to the 1970s due to anthropogenic activity (Painter et al., 2013a; Sun et al., 2020; Grange et al., 2020; Réveillet et al., 2022). However, since the 1980s, emissions have declined (Lim et al., 2017; Kang et al., 2020), largely due to reduced traffic-related pollution, leading to a downward trend in BC deposition (Kutzner et al., 2018; Gidden et al., 2019). Despite this decline, the specific impact of reduced BC deposition on snow cover has yet to be fully quantified, and its contribution to the observed snowpack decline remains uncertain, where complex interactions among BC, radiation, clouds, and snow can have important climatic implications (Tinorua et al., 2024). While the amount of BC deposited on snow has decreased over the last few decades, there is a discernible increase in African dust transport events and resultant

https://doi.org/10.5194/egusphere-2026-4306
Preprint. Discussion started: 21 August 2026

deposition in southern Europe (Varga et al., 2014; Gidden et al., 2019; Salvador et al., 2022; Rostási et al., 2022).

The aforementioned studies, mostly based on remote sensing and modeling, provide valuable broad-scale assessments of LAIs' impacts on snowmelt, but are limited by assumptions and a lack of ground validation. In contrast, this study, conducted in the Central Pyrenees, aims not only to assess the impact of mineral dust and BC on snow but also to quantify their contribution to snowpack evolution.

We hypothesize that, under realistic deposition scenarios in the Pyrenees, African dust can exert an impact on snow properties and melt dynamics comparable to, or even greater than, that of BC. We developed field-based experiments that provide direct observations under controlled conditions to test our hypotheses. Our approach facilitates a more accurate and mechanistic understanding of how specific concentrations of dust and BC affect snow optical properties, melt rates, and energy balance. Thus, experimental measurements are conducted on different days across several weeks, each characterized by varying incoming energy and snow conditions. Therefore, this research presents a preliminary effort to experimentally quantify the role of LAIs in snow processes under real-world conditions.

2. Methodology

2.1 Fieldwork site

The study area is primarily located in two sites within the Pyrenees (Fig. 1). First, the Izas experimental catchment (Revuelto et al., 2017), situated at an altitude of approximately 2054 m. a. s. l., offers optimal conditions for conducting fieldwork throughout the winter. This catchment has been the subject of research for several years, particularly regarding snow and hydrology, providing a solid foundation of data and prior knowledge of the area. Secondly, two specific sectors were selected within the Formigal ski resort: one at 1800 m a.s.l. and the other in the Portalet area at 2200 m a.s.l. These areas, set apart from the main slopes, offer suitable conditions for carrying out field activities without interfering with tourist activity at the resort.

https://doi.org/10.5194/egusphere-2026-4306
Preprint. Discussion started: 21 August 2026

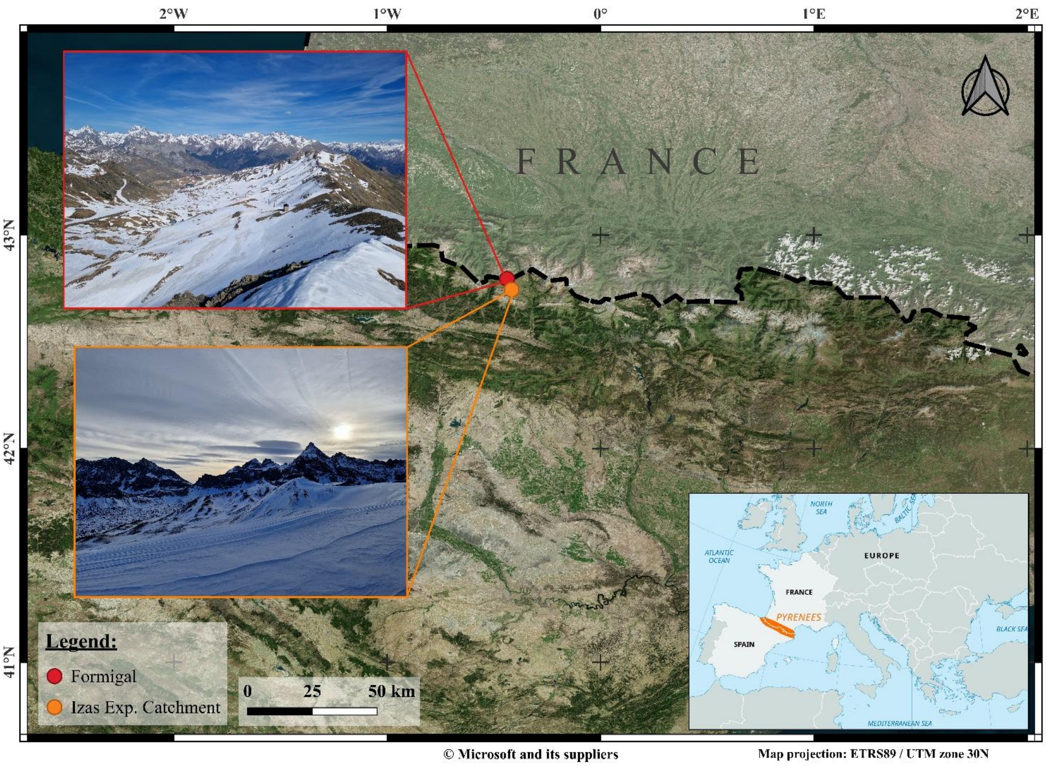

Fig. 1. Location of the two study sites in the Central Pyrenees: Formigal and the Izas Experimental catchment. Microsoft product screen shot reprinted with permission from Microsoft Corporation.

A total of 12 fieldwork days were carried out between January and June 2024 (Table 1). During the peak winter months, activities took place in Formigal and Portalet, because of their easier accessibility, while from May onwards, fieldwork was conducted in Izas due to the presence of snow due to its higher elevation.

Table 1. Compilation of field work days in the two places for the 2024 campaign.

Site	Altitude m.a.s.l	Date	Total days
Izas	2054	8, 22 May	3
		4 June	
Formigal Portalet*	1800-2200	31 January	9
		6, 13, 20 February	
		6, 14, 22 March	
		2*, 19 April	

https://doi.org/10.5194/egusphere-2026-4306
Preprint. Discussion started: 21 August 2026

2.2 Materials used as light absorbing impurities

Soil dust and BC were used for the experiments. Soil dust was collected in Atea (Teruel province, Spain). The final soil sample selected displays a mineral composition like that of the African dust recorded in the Central Pyrenees. (Table S1). The sample was then sieved, and the <20 µm fraction was retained and hereafter referred to as mineral dust. Similarly, BC material was obtained from a local biomass burning incinerator in the Pyrenees. This material was also sieved retaining the <200 µm fraction.

In the laboratory, mineral dust from soil and BC were accurately prepared to run the experiments, by weighing specific amounts using a Mettler Toledo XS105 balance and storing them in 50 ml Falcon tubes. The selected impurity loads were based on the range of mineral dust and BC deposition measured during deposition events previously documented in the Central Pyrenees (Bandrés et al., 2026), ensuring that the experiments represented realistic field conditions (Fig. 2). Accordingly, concentrations equivalent to 2, 5, and 10 g/m^2 were prepared for mineral dust, and 0.1 and 0.2 g/m^2 for BC.

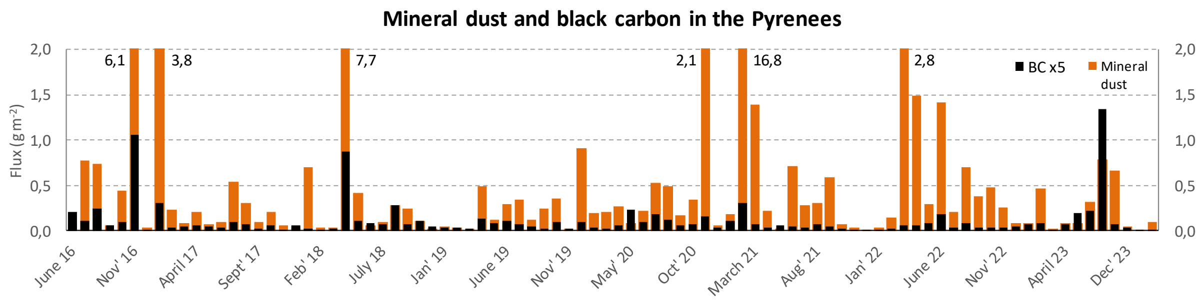

Fig. 2. Monthly flux (in g/m^2) of LAIs (mineral dust and black carbon) recompiled in the Pyrenees 2016-2023. Modified from Bandrés et al. (2026).

2.3 Field work

The experimental setup involved a series of custom mini-lysimeters, each composed of two plastic trays with a surface area of 0.0651 m^2 (0.31 x 0.21 x 0.06 m). The first tray was perforated with consistent spacing to allow meltwater drainage. The first tray also had a lateral wall removed to facilitate sample collection (Fig. 3a). The lower tray was not modified. A flat area with a fixed solar orientation was selected each time, and a snow pit was dug to insert the trays. The upper tray, designated for modification, was filled with a snow block carefully extracted directly from the snowpack. This block was collected with minimal disturbance to preserve its natural structure and aligned with the snow pit surface. The snow block was then weighed using a precision balance (Fig. 3b). Meanwhile, the lower tray was inserted into the resulting cavity in the snow, ensuring it remained level with the surrounding surface. Finally, the upper tray containing the snow block was placed back on top of the lower tray on the snow surface (Fig. 3c). The mini-

https://doi.org/10.5194/egusphere-2026-4306
Preprint. Discussion started: 21 August 2026

lysimeters and their installation (Bandrés, 2026) are very similar to those used by Herrero & Polo (2016) to measure snow evapotranspiration.

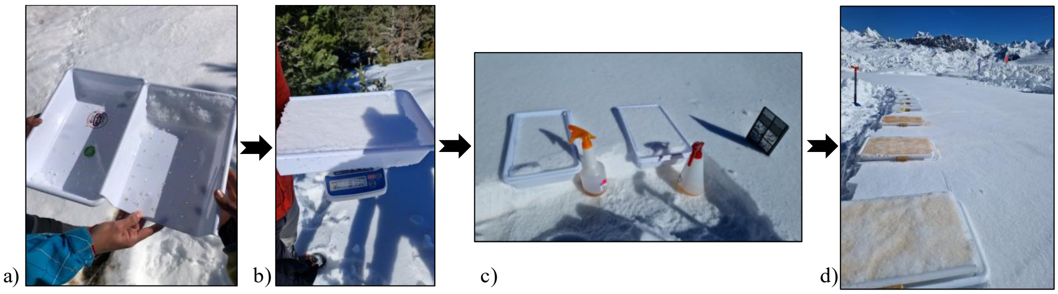

Fig. 3. (a) Twin setup of mini-lysimeters used in the experiments; (b) extraction and weighing of the snow block prior to placement; (c) mini-lysimeters positioned in the snow pit prior to applying the impurities with the spray technique; and (d) experimental setup of mini-lysimeters containing different impurity types and concentrations.

Once the snow samples were properly positioned along the snow pit, the doping procedure was initiated. Each pre-weighted dose of impurities, previously stored in Falcon tubes, was mixed with 20 ml of ethanol to facilitate homogeneous dispersion over the snow surface using a spray bottle. Ethanol was chosen instead of water due to its high volatility, which reduces alteration in the snow's physical and optical properties. The selected concentrations represented realistic African dust deposition events previously recorded in the Pyrenees (2, 5, and 10 g/m^2 for low, medium, and high levels, respectively) as well as typical BC values of 0.1 and 0.2 g/m^2 (Fig. 2). The doping was applied evenly across the surface of each mini-lysimeter (Fig. 3d). For control purposes, one or two trays per session were left untreated (BLK), either completely clean or treated with ethanol only. The same aerosol concentrations were also applied to adjacent undisturbed snow surfaces (the plots), allowing parallel measurements that could not be conducted within the trays.

When possible, on certain days, the same impurity concentrations were replicated in both the trays and the field plots to assess potential variability. Simultaneously, meteorological data were collected using a portable weather station (HOBO U30) installed next to the experimental setup. The station continuously recorded 10-minute averaged measurements of air temperature, relative humidity, incoming solar radiation, and wind speed and direction, to characterize the local atmospheric conditions prevailing at the experimental site.

Measurements of the snow's optical properties began (Fig. S1), including surface broadband albedo on clean, undisturbed snow using a ROX hyperspectral radiometer (JB Hyperspectral Devices, Düsseldorf, Germany), which measures reflectance over the 400-900 nm spectral range corresponding to the instrument's optimal operating range, with a spectral resolution of approximately 1.5 nm. Surface broadband albedo was subsequently measured on each of the trays and plots. Additionally, LWC was measured using an A2

https://doi.org/10.5194/egusphere-2026-4306
Preprint. Discussion started: 21 August 2026

Photonics WISe sensor (A2 Photonic Sensors, 2019) with a well-constrained measurement volume of 325 cm^3, and SSA was assessed using the A2 Photonics IceCube (Martin & Schneebeli, 2023) on nearby undisturbed snow.

After 3-4 h of exposure (with the exact duration recorded for each experimental date), the same snowpack variables initially acquired were re-measured to assess changes over time. Broadband albedo was assessed both on the trays and the plots, while LWC and SSA were measured on undisturbed snow and on the plots. Snow wetness classes were defined following the International Classification for Seasonal Snow on the Ground (ICSSG; Fierz et al., 2009) based on volumetric LWC, distinguishing dry (0%), moist (>0-3%), wet (>3-8%), very wet (>8-15%), and soaked (>15%) snow. Additionally, the total amount of meltwater collected from each tray was recorded in grams.

A summary of the field campaigns conducted throughout the 2024 snow season, including experimental dates, impurity treatments, replicate measurements, and deployed instrumentation, is provided in Fig. S2.

2.4 Meteorological forcing, energy-balance modelling and statistical analysis

Meteorological data for the Formigal and Izas experiments were obtained from the portable weather station and the Izas weather station (Revuelto et al., 2017), respectively. These data were used to force the Factorial Snow Model (FSM2) developed by Essery (2025), which simulated the surface energy balance for each experiment. Model inputs included standard meteorological variables together with the initial physical state of the snowpack, such as snow depth, albedo, grain size, LWC, and snow temperature. Downward longwave radiation under clear-sky conditions was estimated using the parameterization of Herrero & Polo (2012), while the remaining snow variables were derived from field measurements and sensor observations collected during each experiment.

A multiple linear regression model was used to analyze melt percentage. Incoming energy during the experiments, initial snow temperature, LAI load (defined as the surface mass loading of LAIs added to the snow surface, in g/m^2, including both mineral dust and BC additions, with BLK samples assigned a load of 0 g/m^2), initial LWC, and initial SSA were considered as candidate predictors. Predictor selection was performed using a bidirectional stepwise procedure, with all candidate models fitted to the same complete-case dataset. Forward and backward selection were also performed as sensitivity analyses and retained the same final model. The predictors included in the selected model were subsequently standardized to zero mean and unit variance to calculate standardized regression coefficients and compare their relative contributions to melt variability. The same procedure was repeated separately for the mineral dust + BLK and BC + BLK subsets.

https://doi.org/10.5194/egusphere-2026-4306
Preprint. Discussion started: 21 August 2026

Finally, to evaluate whether the responses induced by LAIs exceeded the variability among replicate measurements, a signal-to-noise ratio (SNR) was calculated for melt, albedo, LWC, and SSA. For each replicated treatment, the signal was defined as the absolute difference between the mean treatment response and the corresponding BLK control, while the noise was defined as the standard deviation among treatment replicates.

3. Results

3.1. *Meteorological and snowpack conditions during experimental campaigns*

The experiments were conducted under diverse meteorological and initial snow conditions. Fig. 4 shows the daily average values of air temperature, snow depth, and accumulated precipitation (rain or snowfall) from January 15 to June 15, 2024 in Izas experimental catchment. Air temperatures during the experiments ranged from colder days such as March 6 (2.3 ºC) and April 2 (2.4 ºC), to significantly warmer conditions observed on March 22 (12.2 ºC) and June 4 (12.8 ºC). The greatest snow depth was recorded on April 2, reaching approximately 2 meters following nearly a week of continuous snowfall. Fresh snow conditions were reflected in the low snow densities measured during that day (0.180 kg/m^3), as well as on March 6 (0.210 kg/m^3) and April 19 (0.210 kg/m^3). In situ measurements of solar radiation also showed strong variability throughout the study, with average values during the 4-hour observation periods ranging from 337 W/m^2 on February 6 to peaks of 1240 W/m^2 on May 8 and 1160 W/m^2 on June 4.

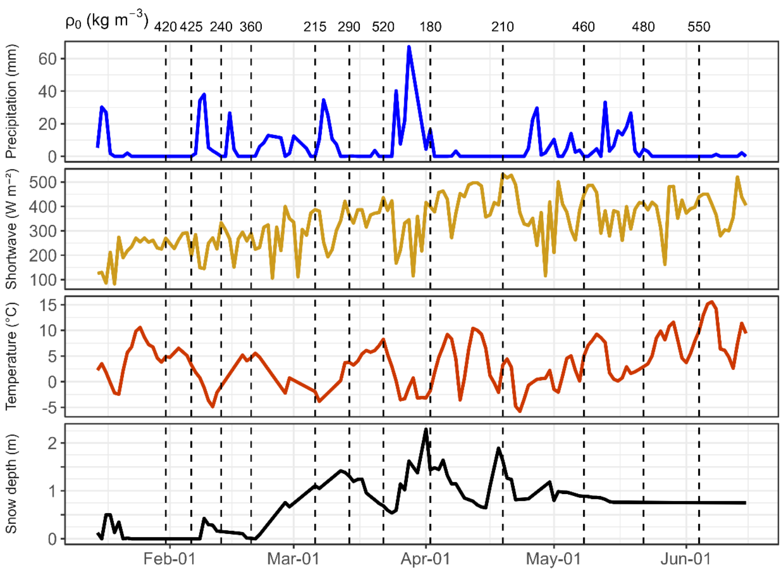

Fig. 4. Time series displaying daily average values of accumulated precipitation (mm), shortwave radiation (W/m^2), temperature (ºC) and snow depth (m) during the study period in 2024. The

https://doi.org/10.5194/egusphere-2026-4306
Preprint. Discussion started: 21 August 2026

dashed lines correspond to each of the twelve experimental dates. Above each line is set the value of the initial snow density, measured in situ. Meteorological and snow data were obtained from the Izas experimental catchment.

3.2. Effects of LAIs on snow optical and physical properties

3.2.1. Albedo

Broadband albedo was derived from field measurements taken directly over each mini-lysimeter and plot at a consistent height (0.5 m), and then averaged for the entire wavelength range (from 400 to 900 nm). Fig. 5 illustrates the impact of LAIs on snow broadband albedo across the different experimental days depicted by their mean incoming energy. As expected, albedo decreases systematically with increasing impurity concentration, with the most substantial reductions observed for the highest mineral dust load (10 g/m^2). Notably, in most cases, the medium mineral dust concentration (5 g/m^2) results in similar or even greater albedo reductions (0.2-0.3) than the high BC load (0.2 g/m^2), reinforcing a non-linear response: doubling the concentration of impurities does not produce a proportional decrease in albedo. Data points associated with lower incoming energy correspond to early- and mid-winter experiments, while those with higher incoming energy values align with late-season experiments.

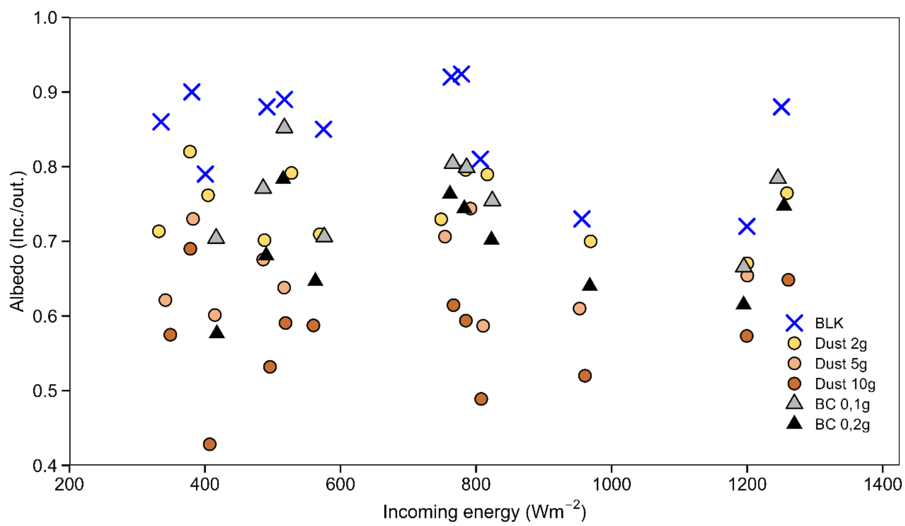

Fig. 5. Relationship between snow albedo and incoming energy (W/m^2) for control conditions (BLK) and snow treated with mineral dust (2, 5, and 10 g/m^2) and BC (0.1 and 0.2 g/m^2).

The average initial broadband albedo across all experiment days was 0.85. The addition of impurities led to a clear and progressive decrease in spectral albedo. For mineral dust, mean albedo values dropped to 0.75 at 2 g/m^2, 0.66 at 5 g/m^2 and 0.57 at 10 g/m^2. In the case of BC, average values were slightly higher: 0.76 at 0.1 g/m^2 and 0.69 at 0.2 g/m^2,

https://doi.org/10.5194/egusphere-2026-4306
Preprint. Discussion started: 21 August 2026

indicating a less pronounced reduction compared to mineral dust, despite concentrations being an order of magnitude lower.

Differences in broadband albedo were observed after the initial doping of the mini-lysimeters and after the 3-4 h experimental period (Fig. 6). LAIs-treated samples show lower albedo values and, in most cases, larger reductions than BLK, with the response modulated by both experimental date and initial snow density (see Table S2).

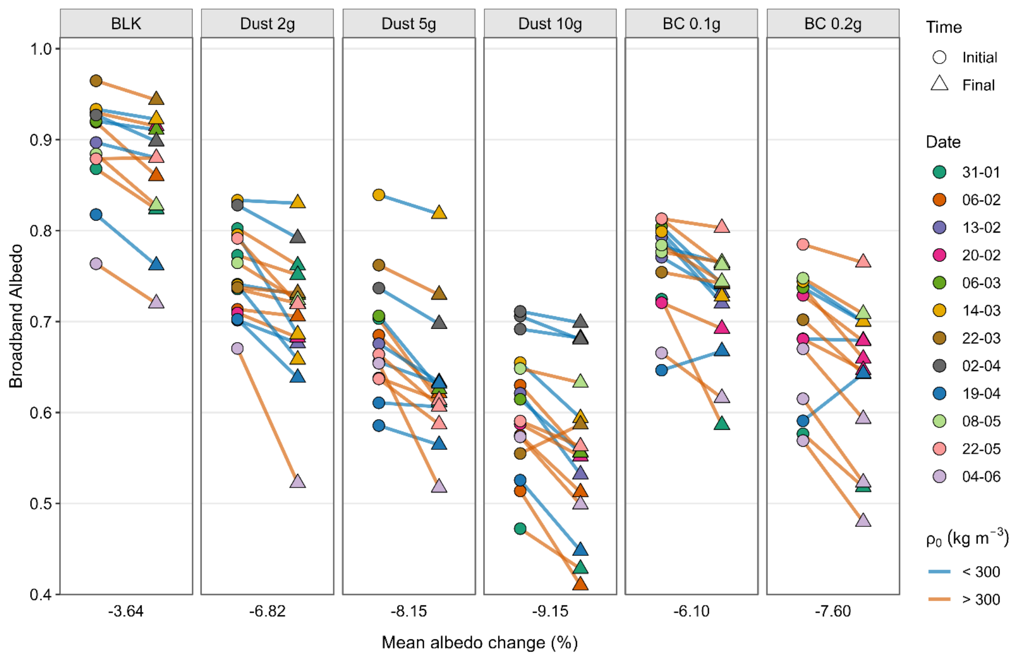

Fig. 6. Initial and final broadband albedo measured in mini-lysimeter experiments for clean snow (BLK), mineral dust additions, and BC additions. Circles indicate initial albedo and triangles final albedo; paired points are connected by lines. Point colors identify the experimental date, while line colors indicate initial snow density classes, $\rho_0 < 300$ kg/m^3 and $\rho_0 > 300$ kg/m^3. The mean initial-to-final albedo change for each treatment is shown below its corresponding panel.

Broadband albedo decreased during the 3-4 h experiments in both clean and LAIs-treated snow. The mean albedo reduction was -3.64% in BLK, and increased to -6.82, -8.15 and -9.15% for the 2, 5 and 10 g/m^2 mineral dust treatments, respectively, and to -6.10 and -7.60% for the 0.1 and 0.2 g/m^2 BC treatments. Relative to the BLK measured on the same day, the largest additional reductions occurred on 4 June for 2 and 5 g/m^2 mineral dust, on 31 January for 0.1 g/m^2 BC, and on 13 February for 10 g/m^2 mineral dust. The response also depended on the initial snow state as can be observed for the two snow density groups: 10 g/m^2 mineral dust produced a stronger response in less-dense snow.

https://doi.org/10.5194/egusphere-2026-4306
Preprint. Discussion started: 21 August 2026

3.2.2 Specific surface area

A similar reduction trend is observed in the SSA when comparing control samples with those affected by impurities, although the non-linear nature of the response is even more evident. SSA tends to decrease as impurity concentrations increases; however, the differences between concentrations and impurity types are not always clearly distinguishable. The most perceptible pattern is the marked reduction of SSA in fresh snow (e.g. $\rho_0 = 0.18$ kg/m^3 with SSA = 30 m^2/kg and $\rho_0 = 0.21$ kg/m^3 with SSA = 18 m^2/kg) following the deposition of impurities, as illustrated in Fig. 7.

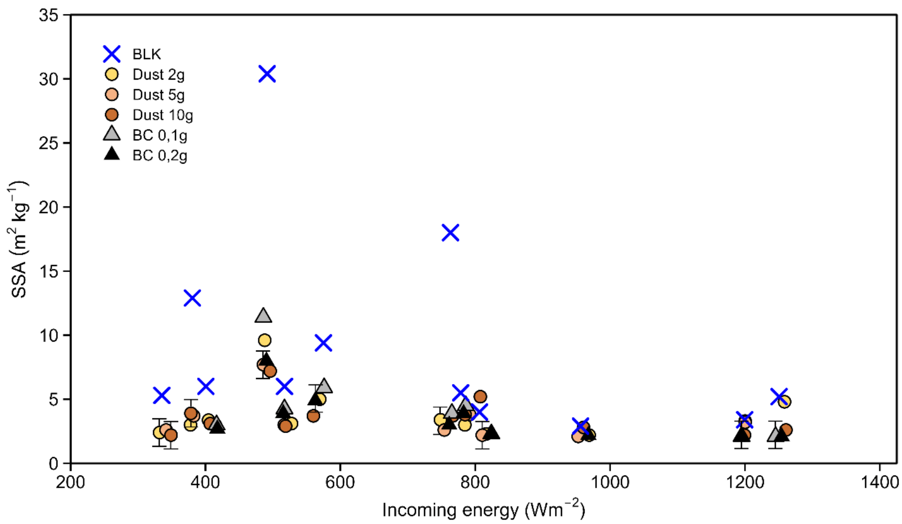

Fig. 7. Relationship between SSA (m^2/kg) and incoming energy (W/m^2) for the control (BLK) and snow treated with mineral dust (2, 5, and 10 g/m^2) and BC (0.1 and 0.2 g/m^2). Error bars indicate the standard deviation of replicate measurements (n = 3), where available.

The average initial SSA across all field experiments was 9.18 m^2/kg. In samples doped with mineral dust, SSA values decreased to 3.81 m^2/kg at 2 g/m^2, 3.69 m^2/kg at 5 g/m^2, and 3.61 m^2/kg at 10 g/m^2. For samples treated with BC, SSA values were 4.36 m^2/kg at 0.1 g/m^2 and 3.64 m^2/kg at 0.2 g/m^2. In most cases, when impurities are present in the samples, SSA drops below 5 m^2/kg. The data confirm a reduction in SSA due to the presence of LAIs, especially when the snow is fresh (less dense in our case study) and more reactive to changes, where the snow structure is more sensitive to impurity-driven metamorphism, though the response is non-linear and depends on these initial snow conditions.

https://doi.org/10.5194/egusphere-2026-4306
Preprint. Discussion started: 21 August 2026

3.2.3 Liquid water content

LWC increased markedly throughout the season in all impurity-treated samples compared to the controls (Fig. 8). Under low-energy conditions and in presence of LAIs, LWC levels reached values typically associated with late-season snowpacks. The graph reveals that on low-incoming-energy days, LWC in control samples remains close to 1%. Once radiation exceeds 800 W/m^2, LWC in controls often surpasses 5%. Only in two cases does LWC exceed 15%, both under the highest mineral dust concentration, followed by BC. In addition, seasonal averages show a clear progression: while the control samples had an average LWC of just 3.1%, even the lowest mineral dust concentration (2 g/m^2), raised it to 6.2%, and the highest (10 g/m^2), reached 10.1%. BC treatments showed intermediate values, 6.8% at 0.1 g/m^2 and 7.8% at 0.2 g/m^2, confirming that mineral dust has a stronger melting effect under comparable conditions. Among all measured variables, LWC showed the highest variability across replicates, likely due to compounding uncertainties from both the instrumentation and the snow density estimation used in its calculation. However, a clear and consistent pattern emerges in two directions: LWC increases both with advancing season and with higher impurity concentrations (see Fig. S3).

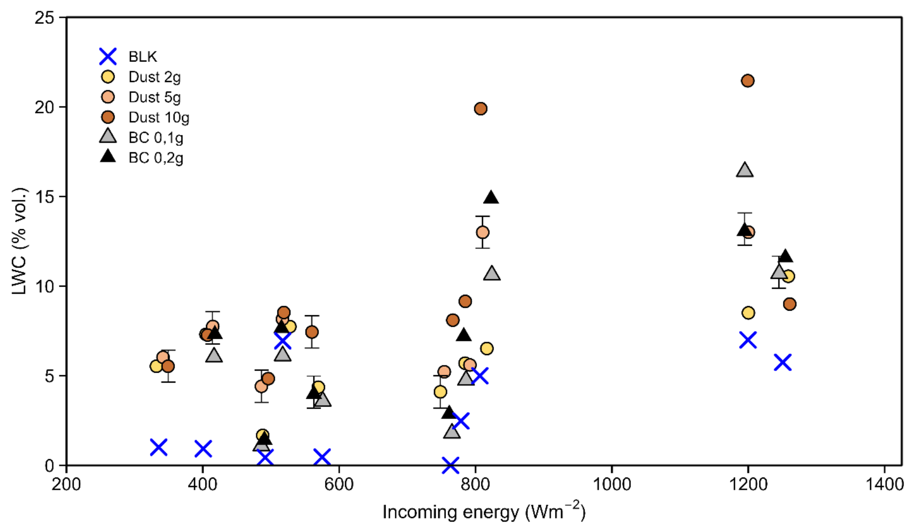

Fig. 8. Relationship between LWC (% vol.) and incoming energy (W/m^2) for the control (BLK) and snow treated with mineral dust (2, 5, and 10 g/m^2) and BC (0.1 and 0.2 g/m^2). Error bars indicate the standard deviation of replicate measurements (n = 3), where available.

3.2.4 Meltwater from snow samples

Meltwater shows that even small amounts of mineral dust can significantly accelerate melting, often doubling melt rates and surpassing the impact of higher BC concentrations (Fig. 9). The fitted linear trends for BLK, mineral dust 5 g/m^2, and BC 0.1 g/m^2 highlight this contrast. Control samples consistently exhibited the lowest melt percentages, even

https://doi.org/10.5194/egusphere-2026-4306
Preprint. Discussion started: 21 August 2026

under high radiation levels, rarely exceeding 50% of the initial snow sample mass. In fact, during many field days, the control snow remained mostly unmelted, while snow with impurities showed substantial melt. BC treatments displayed intermediate behavior, enhancing melt compared to controls but generally resulting in lower melt percentages than mineral dust. However, considerable variability was observed between experiments conducted on different days, highlighting the role of initial snow (whether fresh or metamorphosed) and meteorological conditions. For example, on warmer, sunnier days, even low doses of impurities led to rapid melt, while on colder or cloudier days, the same concentrations had much less effect.

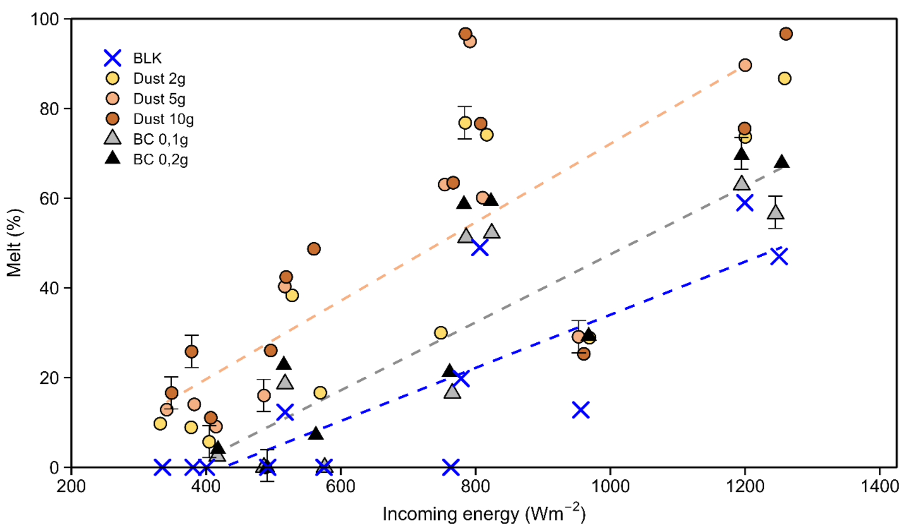

Fig. 9. Effect of LAIs on cumulative snowmelt. Percentage of cumulative snow mass melt, measured from the mini-lysimeters, plotted as a function of incoming energy (W/m^2) for the control and for snow with mineral dust and BC additions. Dashed lines show linear trends for BLK, dust at 5 g/m^2 and BC at 0.1 g/m^2. Error bars indicate the standard deviation of replicate measurements (n = 3), where available.

Melt response showed seasonal evolution, with low values in winter and higher melt fractions in spring and early summer. A summary of the melt percentages recorded throughout the season for each impurity treatment is provided in Fig. S4. On average over the experimental season, cumulative melt was lowest in the BLK treatment (16.7%), increased under BC additions (28.9% for BC 0.1 g/m^2 and 34.0% for BC 0.2 g/m^2), and reached the highest values in the dust treatments, with 37.5%, 42.9% and 50.4% for mineral dust. The BLK trend showed the lowest slope, whereas the 5 g/m^2 mineral dust trend was much steeper and remained consistently above both BLK and BC 0.1 g/m^2 across the observed energy range. The fitted mineral dust (5 g/m^2) response was approximately two to three times higher than BLK and about 30-50% higher than BC (0.1 g/m^2), particularly under intermediate to high energy conditions.

https://doi.org/10.5194/egusphere-2026-4306
Preprint. Discussion started: 21 August 2026

3.2.5 Multiple regression analysis of melt dynamics

Multiple regression analysis was used to determine the relative influence of initial conditions and impurity load on melt percentage. For the complete dataset, stepwise selection retained incoming energy, initial snow temperature and LAI load, whereas initial LWC and SSA did not improve model performance and were therefore excluded. The model which shows the more accurate result was:

$$Melt\ (\%) = 2.28 + 0.072 \cdot Inc.Energy + 9.66 \cdot Tsnow_0 + 3.01 \cdot LAI\ load$$

The global model explained 81% of the variance in melt percentage (adjusted $R^2 = 0.81$, $p < 0.001$), and all retained predictors had positive and significant effects (Fig. 10). Standardized coefficients showed that incoming energy was the dominant predictor ($\beta_{energy} = 0.70$), followed by initial snow temperature ($\beta_{Tsnow0} = 0.37$) and LAI load ($\beta_{LAIs} = 0.35$).

For the mineral dust + BLK subset, stepwise selection retained incoming energy, initial snow temperature and dust load, yielding a model that explained 78% of the variance in melt percentage (adjusted $R^2 = 0.78$, $p < 0.001$). Incoming energy had the largest standardized effect ($\beta_{energy} = 0.67$), followed by initial snow temperature ($\beta_{Tsnow0} = 0.37$) and mineral dust load ($\beta_{dust} = 0.32$).

For the BC + BLK subset, the selected model additionally retained initial LWC and explained 87% of the variance (adjusted $R^2 = 0.87$, $p < 0.001$). Incoming energy remained the dominant predictor ($\beta_{energy} = 0.59$), followed by initial LWC ($\beta_{LWC} = 0.29$), initial snow temperature ($\beta_{Tsnow0} = 0.21$) and BC load ($\beta_{BC} = 0.15$); all effects were positive and significant.

https://doi.org/10.5194/egusphere-2026-4306
Preprint. Discussion started: 21 August 2026

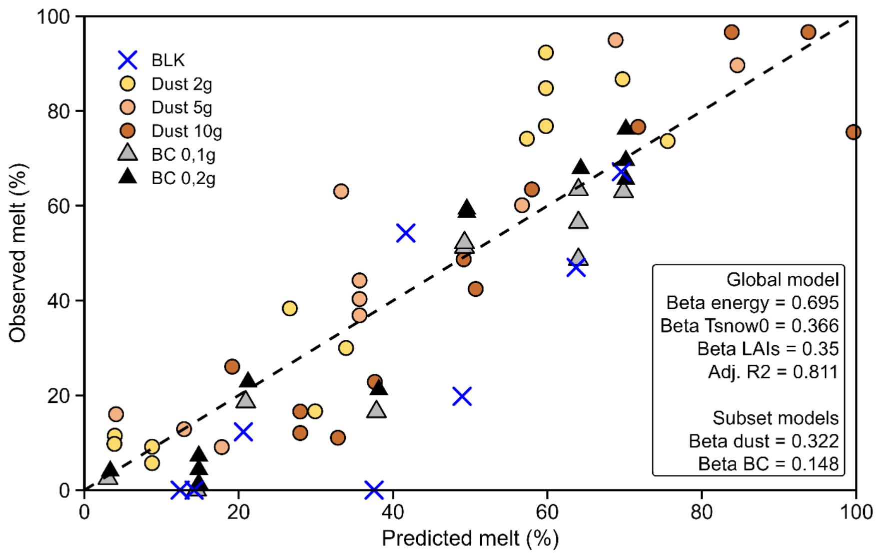

Fig. 10. Observed versus predicted melt percentage for BLK, mineral dust and BC treatments using the stepwise-selected multiple regression model. The dashed line represents the 1:1 relationship. The inset reports standardized regression coefficients for the global model and the impurity-load coefficients obtained from the separate mineral dust + BLK and BC + BLK subset models.

Finally, during the experimental campaign, replicate measurements were performed on several sampling dates for selected LAI load. To assess whether the treatment-induced responses exceeded the variability among replicates, a signal-to-noise ratio (SNR) was calculated. Overall, replicate variability was low and substantially smaller than the changes induced by LAIs. The resulting SNR values, therefore, indicate that the main treatment responses, particularly with mineral dust, were robust and distinguishable from replicate-level variability. (See 7.1 in supplementary material).

4. Discussion

Using realistic aerosol deposition scenarios (Pey et al., 2020; Bandrés et al., 2026), we have designed an experimental approach to quantify the impacts on snow albedo, specific surface area, liquid water content and melt in seasonal snowpacks after the exposition to controlled amounts of two types of LAIs, mineral dust and BC, in contrasted snow and meteorological conditions. The experimental results show that higher impurity concentrations lead to greater reductions in albedo, although the relationship is not linear. While increased concentrations of LAIs generally lead to lower albedo values, the extent of the reduction varies depending on multiple factors. For instance, the same concentration of impurities applied on different days yielded varying albedo responses, suggesting a significant influence of intrinsic snowpack factors such as snow microstructure, grain morphology, internal water saturation, temperature, and other environmental variables such as incident shortwave radiation. Notably, mineral dust exhibited a more pronounced effect on albedo reduction compared to BC at intermediate concentrations. This finding supports previous work (e.g., Dumont et al., 2014; Painter et al., 2018), in which mineral dust under specific conditions induced greater radiative forcing than BC. According to Skiles et al. (2018), BC is the most efficient light-absorbing particle on a mass basis, but in many mountain regions mineral dust exerts a stronger overall impact on snowmelt due to its much higher deposition loads and its tendency to accumulate at the surface during the melt season. IPCC assessments identify BC deposited on snow and ice as an important factor in albedo reduction and regional radiative forcing, with an estimated forcing increase of 0.10 ± 0.10 W/m^2 for BC in snow (Hansen et al., 2000; Hansen & Nazarenko, 2003; IPCC AR4, Section 2.5.4). However, in southern European mountain ranges such as the Pyrenees, African dust deposition is magnified under certain meteorological circulation patterns giving rise to almost annual large dust-deposition events. As discussed by Pey et al. (2020), the Foehn effect promotes the wash out of dusty air masses from North Africa when encountered the Pyrenees in their northward movement. The same mechanism could be observed in other mountains facing the Mediterranean. This topographically enhanced deposition mechanism, combined with the seasonal susceptibility of the snowpack, amplifies the role of mineral dust over BC in modulating snow properties and melt dynamics. Consequently, in contrast to global-scale assumptions where BC dominates, mineral dust may be the prevailing LAIs in the Pyrenees, reinforcing the need for region-specific assessments in our study area and beyond.

Regarding the changes observed in snow properties, a reduction in SSA and an increase in LWC were consistently observed alongside decreases in albedo. These effects were again clearly modulated by the initial snow conditions (categorized by the snow density) and the stage of seasonal evolution. Several studies demonstrate that increasing liquid water content alters the spectral albedo of snow (Adolph & Wang, 2024) because of increased absorption in the near-infrared and shortwave infrared (NIR-SWIR) wavelengths. While Li & Wu (2025) confirm through modeling that liquid water significantly reduces NIR-SWIR albedo in snowpacks, particularly for smaller grain sizes. In fresh, low-density snow, SSA exhibited a more pronounced decline after impurity deposition due to the transition from dendritic crystals to rounded grains driven by metamorphism (similarly to what is shown in Fig. 7 of this work). This transformation not only reduces the radiative reflectivity but also increases the potential for energy absorption, although with a delayed onset of significant melt due to initially lower internal water saturation and snow temperature, as shown by Domine et al. (2007) and Dang et al. (2016). In contrast, older, more evolved snow with already rounded grains, exhibited minimal further reduction in SSA as noted by Aoki et al. (2003, 2007) and Niwano et al. (2012), because the snowpack had already undergone metamorphism prior to the experiments. In these cases, the primary impact of LAIs was more evident in increased meltwater production and LWC, as these snowpacks were generally warmer and more responsive to additional energy input. Hence, while changes in SSA were limited, the albedo-driven increase in energy absorption translated more directly into meltwater

https://doi.org/10.5194/egusphere-2026-4306
Preprint. Discussion started: 21 August 2026

generation. Our observations reflect the feedback described by Skiles et al. (2018), where LAIs-induced grain growth reduces albedo, increasing energy absorption and further accelerating melt, a process modulated by the initial physical state of the snowpack.

The meltwater collected from mini-lysimeters highlights the strong radiative forcing capacity of mineral dust to melt snow. Even at the lowest concentrations of mineral dust, melt rates frequently doubled those of the control samples. This significant enhancement occurred even under moderate energy input conditions, emphasizing the high efficacy of mineral dust in accelerating snowmelt. In contrast, as happened with albedo, LWC and SSA, BC produced significant, but more moderate changes in meltwater, typically lower than that observed with medium or high mineral dust concentrations. Overall, beta coefficients from regression analyses revealed that LAIs' influence on snowmelt has a similar weight to initial snow temperature of the snowpack, and meteorological conditions that drive the snow energy balance roughly double the role of the concentration of impurities on the snow. However, the relevance of LAIs' impacts is clear under isothermal conditions in denser snowpacks. The separate models indicate that the relative contribution of impurity load was stronger in the mineral dust model than in the BC model. Modeling experiments by Di Mauro et al. (2019) demonstrated that African dust deposition can advance snowmelt by up to 38 days. Similarly, Réveillet et al. (2022) found that the combined effects of mineral dust and BC advanced the snow melt-out date by approximately 17 ± 6 days in the French Alps and the Pyrenees over the 1979-2018 period, relative to simulations of clean snow without LAIs. The previous studies mentioned above have many common findings. Looking forward, the role of LAIs in snowmelt dynamics is expected to rise, particularly under scenarios of intensified African dust transport to mountain regions such as the Pyrenees (Salvador et al., 2022, 2024).

Our experimental design provides valuable insights into how LAIs affect snow dynamics. It enables testing of different types and concentrations of LAIs under comparable meteorological conditions, with results obtained within a single day using relatively portable instrumentation. This approach generates direct observational datasets that are difficult to obtain with conventional field monitoring and provide valuable information for cryospheric research. Nevertheless, this experimental approach involves unavoidable methodological limitations inherent in fieldwork. First, the spatial and temporal resolution is constrained: snow blocks are partially isolated from the natural snowpack in the mini-lysimeters and manipulated, with the experiment lasting only 3-4 h. Additionally, aerosols were dispersed using ethanol because preliminary tests showed that water modified snow properties, particularly surface albedo and LWC. Ethanol evaporates rapidly leaving impurities on the snow surface; it still introduces a non-natural element into the experiment. Some of these limitations could be addressed in future studies. For example, developing dry-deposition techniques to replace ethanol, testing the experimental setup under different slope aspects, or applying the treatments directly to the natural snow surface where meltwater collection is not required. Although our study captures only short-term responses and cannot fully replicate the complexity of long-term and deep snowpack evolution, the dataset is unique and could provide valuable information for validating large-scale models and enhancing understanding of LAI-snow

https://doi.org/10.5194/egusphere-2026-4306
Preprint. Discussion started: 21 August 2026

interactions under realistic impurity loads. At broader scales, airborne or satellite remote sensing technologies are increasingly powerful tools for monitoring snow impurities and melt processes across mountain regions. In this context, hyperspectral cameras mounted on drones and high-resolution satellite products can provide promising information on snow surface properties (Kokhanovsky et al., 2019; Sproles et al., 2020), and the presence of impurities including dust and BC indices.

5. Conclusions

This study provides experimental evidence of the significant impact of light-absorbing impurities (LAIs), particularly African dust and black carbon (BC), on snow surface energy balance and melt dynamics in the Central Pyrenees. Using a mini-lysimeter setup under realistic impurity deposition scenarios, our field experiments consistently showed substantial reductions in broadband albedo (0.2-0.3), decreases in specific surface area (5.5-6.5 m^2/kg), and increases in liquid water content (1.5-2.0%) and meltwater production across a wide range of snow and meteorological conditions.

The experimental approach proved effective for isolating and quantifying the direct effects of LAIs on snow properties under natural environmental conditions. Despite its simplicity and low cost, the setup allowed controlled comparisons between impurity types and concentrations, providing one of the few direct experimental datasets linking aerosol loads to changes in snow metamorphism and melt. Such observations are important for validating snowpack and radiative transfer models, which often ignore or rely on assumptions regarding impurity effects.

The results revealed a clear but non-linear response of snow properties to impurity loading. Higher concentrations of LAIs generally produced stronger impacts, although the magnitude of the response depended strongly on initial snow conditions, including snow microstructure, liquid water content, metamorphic stage, and temperature, as well as on incoming shortwave radiation. Consequently, identical impurity concentrations could produce different responses under different environmental conditions.

Among all measured variables, meltwater production provided the clearest evidence of the radiative forcing exerted by impurities. Mineral dust frequently doubled melt rates relative to clean snow and, in several cases, induced measurable melt while control samples remained stable. Mineral dust consistently produced stronger effects than BC under comparable radiative conditions, even at intermediate concentrations. Considering realistic deposition scenarios in the southern Pyrenees, mineral dust was approximately 50% more effective than BC in reducing albedo and enhancing melt-related processes, including SSA reduction and LWC increase. Thus, despite the greater mass-specific absorptivity of BC, the frequency and magnitude of African dust deposition make mineral dust the dominant impurity affecting snowmelt in the Pyrenees, and other regions affected by mineral dust.

https://doi.org/10.5194/egusphere-2026-4306
Preprint. Discussion started: 21 August 2026

Finally, the dataset highlights the importance of incorporating realistic impurity loads and snow conditions into future snowpack studies. Our efforts provide rough constraints for simulating snowpack evolution. The relevance of these findings will only increase as African dust intrusions are projected to increase in frequency and intensity in southern Europe under climate change, while BC emissions continue to decline. Future work should be two-part: 1) conducting controlled laboratory experiments with a similar design to better constrain melt models, and 2) focus on scaling these observations from point measurements to plot, catchment, and regional scales by integrating field experiments, remote sensing observations, and physically based snow models.

Data and code availability

The data supporting the findings of this study are publicly available at Zenodo: https://doi.org/10.5281/zenodo.22017914 (Bandrés García, 2026). No custom code was developed for this study.

Author contributions

JB led the study, conducted the fieldwork, curated and processed the data, performed the analyses, and prepared the original manuscript. JP and JILM supervised the study and contributed to the fieldwork, data interpretation, formal analysis, and review and editing of the manuscript. EI, FRH, and PDA contributed to the fieldwork and reviewed and edited the manuscript. EAS contributed to data processing and interpretation and reviewed and edited the manuscript. EAG contributed to the formal analysis and reviewed and edited the manuscript. JR contributed to the fieldwork, data processing and interpretation, and review and editing of the manuscript. All authors reviewed and approved the final version of the manuscript.

Competing interests

The authors declare that they have no conflict of interest.

Acknowledgements

JB gratefully acknowledges the University of Zaragoza for support during doctoral studies.

https://doi.org/10.5194/egusphere-2026-4306
Preprint. Discussion started: 21 August 2026

Financial support

The first author was supported by an FPI predoctoral grant associated with the MARGISNOW project (PID2021-124220OB-I00) funded by the Spanish Ministry of Science and Innovation. This research received support from POSAHPI actions (AEI, PID2019-108101RB-I00, PID2022-143146OB-I00), ASAH-AS (OAPN 2021, reference 2799/2021), and SNOWDUST (AEI, TED2021-130114B-I00).

Bibliography

A2 Photonic Sensors: WISe – Snow liquid water content sensor – User Manual, A2 Photonics Sensors, Grenoble, France, 2019.

Adolph, A. C., & Wang, J. (2024, December). Analytical modeling of the effect of liquid water on the spectral albedo of snow [Conference presentation abstract]. *AGU Annual Meeting 2024*, Washington, DC, United States.

Aoki, T., Hachikubo, A., & Hori, M. (2003). Effects of snow physical parameters on shortwave broadband albedos. *Journal of Geophysical Research: Atmospheres*, *108*(D19). https://doi.org/10.1029/2003jd003506

Arimoto, R. (2001). Eolian dust and climate: Relationships to sources, tropospheric chemistry, transport and deposition. *Earth-Science Reviews*, *54*(1–3), 29–42. https://doi.org/10.1016/s0012-8252(01)00040-x

Arnalds, O., Dagsson-Waldhauserova, P., & Olafsson, H. (2016). The Icelandic volcanic aeolian environment: Processes and impacts — A review. *Aeolian Research*, *20*, 176–195. https://doi.org/10.1016/j.aeolia.2016.01.004

Bandrés, J. Assessing impurity-driven snowmelt with mini-lysimeters. *Nat Rev Earth Environ* **7**, 411 (2026). https://doi.org/10.1038/s43017-026-00799-7

Bandrés, J., López-Moreno, J. I., Salvador, P., & Pey, J. (2026). Chemistry and sources of atmospheric aerosols deposited in the Central Pyrenees in the period 2016–2023, with a focus on African dust events occurred during cold season. *Atmospheric Research*, *331*, 108686. https://doi.org/10.1016/j.atmosres.2025.108686

Bandrés García, J. (2026). Dataset of "Quantifying the impact of Light Absorbing Impurities on snow properties and melting using mini-lysimeters in the Central Pyrenees". Zenodo [data set]. https://doi.org/10.5281/zenodo.22017914

Barkan, J., Alpert, P., Kutiel, H., & Kishcha, P. (2005). Synoptics of dust transportation days from Africa toward Italy and central Europe. *Journal of Geophysical Research: Atmospheres*, *110*(D7). https://doi.org/10.1029/2004jd005222

Barkan, J., Kutiel, H., Alpert, P., & Kishcha, P. (2004). Synoptics of dust intrusion days from the African continent into the Atlantic Ocean. *Journal of Geophysical Research: Atmospheres*, *109*(D8). https://doi.org/10.1029/2003jd004416

Bayle, A., Gascoin, S., Corona, C., Stoffel, M., & Choler, P. (2025). Snow melt-out date (SMOD) change spanning four decades in European temperate mountains at 30 m from Landsat time series. *Scientific Data*, *12*(1). https://doi.org/10.1038/s41597-025-05044-2

Beniston, M., Farinotti, D., Stoffel, M., Andreassen, L. M., Coppola, E., Eckert, N., Fantini, A., Giacona, F., Hauck, C., Huss, M., Huwald, H., Lehning, M., López-Moreno, J.-I., Magnusson, J., Marty, C., Morán-Tejéda, E., Morin, S., Naaim, M., Provenzale, A., … Vincent, C. (2018). The European mountain cryosphere: A review of its current state, trends, and future challenges. *The Cryosphere*, *12*(2), 759–794. https://doi.org/10.5194/tc-12-759-2018

Beniston, M., & Stoffel, M. (2014). Assessing the impacts of climatic change on mountain water resources. *Science of the Total Environment*, *493*, 1129–1137. https://doi.org/10.1016/j.scitotenv.2013.11.122

Bond, T. C., Doherty, S. J., Fahey, D. W., Forster, P. M., Berntsen, T., DeAngelo, B. J., Flanner, M. G., Ghan, S., Kärcher, B., Koch, D., Kinne, S., Kondo, Y., Quinn, P. K., Sarofim, M. C., Schultz, M. G., Schulz, M., Venkataraman, C., Zhang, H., Zhang, S., … Zender, C. S. (2013). Bounding the role of black carbon in the climate system: A scientific assessment. *Journal of Geophysical Research: Atmospheres*, *118*(11), 5380–5552. https://doi.org/10.1002/jgrd.50171

Bond, T. C., Streets, D. G., Yarber, K. F., Nelson, S. M., Woo, J., & Klimont, Z. (2004). A technology-based global inventory of black and organic carbon emissions from combustion. *Journal of Geophysical Research: Atmospheres*, *109*(D14). https://doi.org/10.1029/2003jd003697

https://doi.org/10.5194/egusphere-2026-4306
Preprint. Discussion started: 21 August 2026

Dagsson-Waldhauserova, P., Arnalds, O., Olafsson, H., Hladil, J., Skala, R., Navratil, T., Chadimova, L., & Meinander, O. (2015). Snow–Dust Storm: Unique case study from Iceland, March 6–7, 2013. *Aeolian Research*, *16*, 69–74. https://doi.org/10.1016/j.aeolia.2014.11.001

Dang, C., Fu, Q., & Warren, S. G. (2016). Effect of snow grain shape on snow albedo. *Journal of the Atmospheric Sciences*, *73*(9), 3573–3583. https://doi.org/10.1175/jas-d-15-0276.1

Di Mauro, B., Fava, F., Ferrero, L., Garzonio, R., Baccolo, G., Delmonte, B., & Colombo, R. (2015). Mineral dust impact on snow radiative properties in the European Alps combining ground, UAV, and satellite observations. *Journal of Geophysical Research: Atmospheres*, *120*(12), 6080–6097. https://doi.org/10.1002/2015jd023287

Di Mauro, B., Garzonio, R., Rossini, M., Filippa, G., Pogliotti, P., Galvagno, M., Morra di Cella, U., Migliavacca, M., Baccolo, G., Clemenza, M., Delmonte, B., Maggi, V., Dumont, M., Tuzet, F., Lafaysse, M., Morin, S., Cremonese, E., & Colombo, R. (2019). Saharan dust events in the European Alps: Role in snowmelt and geochemical characterization. *The Cryosphere*, *13*(4), 1147–1165. https://doi.org/10.5194/tc-13-1147-2019

Doherty, S. J., Warren, S. G., Grenfell, T. C., Clarke, A. D., & Brandt, R. E. (2010). Light-absorbing impurities in Arctic snow. *Atmospheric Chemistry and Physics*, *10*(23), 11647–11680. https://doi.org/10.5194/acp-10-11647-2010

Domine, F., Taillandier, A. -s., & Simpson, W. R. (2007). A parameterization of the specific surface area of seasonal snow for field use and for models of snowpack evolution. *Journal of Geophysical Research: Earth Surface*, *112*(F2). https://doi.org/10.1029/2006jf000512

Dumont, M., Arnaud, L., Picard, G., Libois, Q., Lejeune, Y., Nabat, P., Voisin, D., & Morin, S. (2017). In situ continuous visible and near-infrared spectroscopy of an alpine snowpack. *The Cryosphere*, *11*(3), 1091–1110. https://doi.org/10.5194/tc-11-1091-2017

Dumont, M., Brun, E., Picard, G., Michou, M., Libois, Q., Petit, J.-R., Geyer, M., Morin, S., & Josse, B. (2014). Contribution of light-absorbing impurities in snow to Greenland's darkening since 2009. *Nature Geoscience*, *7*(7), 509–512. https://doi.org/10.1038/ngeo2180

https://doi.org/10.5194/egusphere-2026-4306
Preprint. Discussion started: 21 August 2026

Essery, R., Mazzotti, G., Barr, S., Jonas, T., Quaife, T., & Rutter, N. (2025). A Flexible Snow Model (FSM 2.1.1) including a forest canopy. *Geoscientific Model Development*, *18*(12), 3583–3605. https://doi.org/10.5194/gmd-18-3583-2025

European state of the climate 2023. (n.d.). Copernicus. Retrieved October 2, 2025, from https://climate.copernicus.eu/esotc/2023

Fayad, A., Gascoin, S., Faour, G., Fanise, P., Drapeau, L., Somma, J., Fadel, A., Al Bitar, A., & Escadafal, R. (2017). Snow observations in Mount Lebanon (2011–2016). *Earth System Science Data*, *9*(2), 573–587. https://doi.org/10.5194/essd-9-573-2017

Fierz, C., Armstrong, R. L., Durand, Y., Etchevers, P., Greene, E., McClung, D. M., Nishimura, K., Satyawali, P. K., & Sokratov, S. A. (2009). *The international classification for seasonal snow on the ground.* IHP-VII Technical Documents in Hydrology No. 83, IACS Contribution No. 1. UNESCO-IHP.

Flanner, M. G., Shell, K. M., Barlage, M., Perovich, D. K., & Tschudi, M. A. (2011). Radiative forcing and albedo feedback from the Northern Hemisphere cryosphere between 1979 and 2008. *Nature Geoscience*, *4*(3), 151–155. https://doi.org/10.1038/ngeo1062

Flanner, M. G., Zender, C. S., Randerson, J. T., & Rasch, P. J. (2007). Present-day climate forcing and response from black carbon in snow. *Journal of Geophysical Research: Atmospheres*, *112*(D11). https://doi.org/10.1029/2006jd008003

Gautam, R., Hsu, N. C., Lau, W. K. -M., & Yasunari, T. J. (2013). Satellite observations of desert dust-induced Himalayan snow darkening. *Geophysical Research Letters*, *40*(5), 988–993. https://doi.org/10.1002/grl.50226

Gidden, M. J., Riahi, K., Smith, S. J., Fujimori, S., Luderer, G., Kriegler, E., van Vuuren, D. P., van den Berg, M., Feng, L., Klein, D., Calvin, K., Doelman, J. C., Frank, S., Fricko, O., Harmsen, M., Hasegawa, T., Havlik, P., Hilaire, J., Hoesly, R., … Takahashi, K. (2019). Global emissions pathways under different socioeconomic scenarios for use in CMIP6: A dataset of harmonized emissions trajectories through the end of the century. *Geoscientific Model Development*, *12*(4), 1443–1475. https://doi.org/10.5194/gmd-12-1443-2019

Ginoux, P., Chin, M., Tegen, I., Prospero, J. M., Holben, B., Dubovik, O., & Lin, S. (2001). Sources and distributions of dust aerosols simulated with the GOCART model. *Journal of Geophysical Research: Atmospheres*, *106*(D17), 20255–20273. https://doi.org/10.1029/2000jd000053

Gobiet, A., Kotlarski, S., Beniston, M., Heinrich, G., Rajczak, J., & Stoffel, M. (2014). 21st century climate change in the European Alps—A review. *Science of the Total Environment*, *493*, 1138–1151. https://doi.org/10.1016/j.scitotenv.2013.07.050

Grange, S. K., Lötscher, H., Fischer, A., Emmenegger, L., & Hueglin, C. (2020). Evaluation of equivalent black carbon source apportionment using observations from Switzerland between 2008 and 2018. *Atmospheric Measurement Techniques*, *13*(4), 1867–1885. https://doi.org/10.5194/amt-13-1867-2020

Greilinger, M., Schauer, G., Baumann-Stanzer, K., Skomorowski, P., Schöner, W., & Kasper-Giebl, A. (2018). Contribution of Saharan dust to ion deposition loads of high alpine snow packs in Austria (1987–2017). *Frontiers in Earth Science*, *6*. https://doi.org/10.3389/feart.2018.00126

Hadley, O. L., & Kirchstetter, T. W. (2012). Black-carbon reduction of snow albedo. *Nature Climate Change*, *2*(6), 437–440. https://doi.org/10.1038/nclimate1433

Hansen, J., & Nazarenko, L. (2003). Soot climate forcing via snow and ice albedos. *Proceedings of the National Academy of Sciences*, *101*(2), 423–428. https://doi.org/10.1073/pnas.2237157100

Hansen, J., Sato, M., Ruedy, R., Lacis, A., & Oinas, V. (2000). Global warming in the twenty-first century: An alternative scenario. *Proceedings of the National Academy of Sciences*, *97*(18), 9875–9880. https://doi.org/10.1073/pnas.170278997

Herrero, J., & Polo, M. J. (2012). Parameterization of atmospheric longwave emissivity in a mountainous site for all sky conditions. *Hydrology and Earth System Sciences*, *16*(9), 3139–3147. https://doi.org/10.5194/hess-16-3139-2012

Herrero, J., & Polo, M. J. (2016). Evaposublimation from the snow in the Mediterranean mountains of Sierra Nevada (Spain). *The Cryosphere*, *10*(6), 2981–2998. https://doi.org/10.5194/tc-10-2981-2016

Jones, H. A. (1913). EFFECT OF DUST ON THE MELTING OF SNOW. *Monthly Weather Review*, *41*(4), 599–599. https://doi.org/10.1175/1520-0493(1913)41<599a:eodotm>2.0.co;2

https://doi.org/10.5194/egusphere-2026-4306
Preprint. Discussion started: 21 August 2026

Kang, S., Zhang, Y., Qian, Y., & Wang, H. (2020). A review of black carbon in snow and ice and its impact on the cryosphere. *Earth-Science Reviews*, *210*, 103346. https://doi.org/10.1016/j.earscirev.2020.103346

Klein, H., Nickovic, S., Haunold, W., Bundke, U., Nillius, B., Ebert, M., Weinbruch, S., Schuetz, L., Levin, Z., Barrie, L. A., & Bingemer, H. (2010). Saharan dust and ice nuclei over Central Europe. *Atmospheric Chemistry and Physics*, *10*(21), 10211–10221. https://doi.org/10.5194/acp-10-10211-2010

Kokhanovsky, A., Lamare, M., Danne, O., Brockmann, C., Dumont, M., Picard, G., Arnaud, L., Favier, V., Jourdain, B., Le Meur, E., Di Mauro, B., Aoki, T., Niwano, M., Rozanov, V., Korkin, S., Kipfstuhl, S., Freitag, J., Hoerhold, M., Zuhr, A., … Box, J. (2019). Retrieval of snow properties from the sentinel-3 ocean and land colour instrument. *Remote Sensing*, *11*(19), 2280. https://doi.org/10.3390/rs11192280

Kutzner, R. D., von Schneidemesser, E., Kuik, F., Quedenau, J., Weatherhead, E. C., & Schmale, J. (2018). Long-term monitoring of black carbon across Germany. *Atmospheric Environment*, *185*, 41–52. https://doi.org/10.1016/j.atmosenv.2018.04.039

Laternser, M., & Schneebeli, M. (2003). Long-term snow climate trends of the Swiss Alps (1931–99). *International Journal of Climatology*, *23*(7), 733–750. https://doi.org/10.1002/joc.912

Li, F., & Wu, K. (2025). Improvement of snow albedo simulation considering water content. *Remote Sensing*, *17*(23), 3899. https://doi.org/10.3390/rs17233899

Lim, S., Faïn, X., Ginot, P., Mikhalenko, V., Kutuzov, S., Paris, J.-D., Kozachek, A., & Laj, P. (2017). Black carbon variability since preindustrial times in the eastern part of Europe reconstructed from Mt. Elbrus, Caucasus, ice cores. *Atmospheric Chemistry and Physics*, *17*(5), 3489–3505. https://doi.org/10.5194/acp-17-3489-2017

Liu, E. J., Cashman, K. V., Beckett, F. M., Witham, C. S., Leadbetter, S. J., Hort, M. C., & Guðmundsson, S. (2014). Ash mists and brown snow: Remobilization of volcanic ash from recent Icelandic eruptions. *Journal of Geophysical Research: Atmospheres*, *119*(15), 9463–9480. https://doi.org/10.1002/2014jd021598

López-Moreno, J. I., Gascoin, S., Herrero, J., Sproles, E. A., Pons, M., Alonso-González, E., Hanich, L., Boudhar, A., Musselman, K. N., Molotch, N. P., Sickman, J., &

Pomeroy, J. (2017). Different sensitivities of snowpacks to warming in Mediterranean climate mountain areas. *Environmental Research Letters*, *12*(7), 074006. https://doi.org/10.1088/1748-9326/aa70cb

Marcolini, G., Bellin, A., Disse, M., & Chiogna, G. (2017). Variability in snow depth time series in the Adige catchment. *Journal of Hydrology: Regional Studies*, *13*, 240–254. https://doi.org/10.1016/j.ejrh.2017.08.007

Marín-Beltrán, I., Bandrés, J., Domínguez-Aguilar, P., Pey, J., Revuelto, J., & López-Moreno, J. I. (2026). Dark microplastics trigger changes on snow metamorphism that depends on the snow initial density. *iScience*, *29*(3), 114829. https://doi.org/10.1016/j.isci.2026.114829

Martin, J., & Schneebeli, M. (2023). Impact of the sampling procedure on the specific surface area of snow measurements with the IceCube. *The Cryosphere*, *17*(4), 1723–1734. https://doi.org/10.5194/tc-17-1723-2023

Musselman, K. N., Addor, N., Vano, J. A., & Molotch, N. P. (2021). Winter melt trends portend widespread declines in snow water resources. *Nature Climate Change*, *11*(5), 418–424. https://doi.org/10.1038/s41558-021-01014-9

Niwano, M., Aoki, T., Kuchiki, K., Hosaka, M., & Kodama, Y. (2012). Snow Metamorphism and Albedo Process (SMAP) model for climate studies: Model validation using meteorological and snow impurity data measured at Sapporo, Japan. *Journal of Geophysical Research: Earth Surface*, *117*(F3). https://doi.org/10.1029/2011jf002239

Painter, T. H., Bryant, A. C., & Skiles, S. M. (2012). Radiative forcing by light absorbing impurities in snow from MODIS surface reflectance data. *Geophysical Research Letters*, *39*(17). https://doi.org/10.1029/2012gl052457

Painter, T. H., Flanner, M. G., Kaser, G., Marzeion, B., VanCuren, R. A., & Abdalati, W. (2013a). End of the Little Ice Age in the Alps forced by industrial black carbon. *Proceedings of the National Academy of Sciences*, *110*(38), 15216–15221. https://doi.org/10.1073/pnas.1302570110

Painter, T. H., Seidel, F. C., Bryant, A. C., McKenzie Skiles, S., & Rittger, K. (2013b). Imaging spectroscopy of albedo and radiative forcing by light-absorbing impurities in mountain snow. *Journal of Geophysical Research: Atmospheres*, *118*(17), 9511–9523. https://doi.org/10.1002/jgrd.50520

Painter, T. H., Skiles, S. M., Deems, J. S., Brandt, W. T., & Dozier, J. (2018). Variation in rising limb of colorado river snowmelt runoff hydrograph controlled by dust radiative forcing in snow. *Geophysical Research Letters*, *45*(2), 797–808. https://doi.org/10.1002/2017gl075826

Pendergrass, A. G., Knutti, R., Lehner, F., Deser, C., & Sanderson, B. M. (2017). Precipitation variability increases in a warmer climate. *Scientific Reports*, *7*(1). https://doi.org/10.1038/s41598-017-17966-y

Pey, J., Larrasoaña, J. C., Pérez, N., Cerro, J. C., Castillo, S., Tobar, M. L., de Vergara, A., Vázquez, I., Reyes, J., Mata, M. P., Mochales, T., Orellana, J. M., & Causapé, J. (2020). Phenomenology and geographical gradients of atmospheric deposition in southwestern Europe: Results from a multi-site monitoring network. *Science of the Total Environment*, *744*, 140745. https://doi.org/10.1016/j.scitotenv.2020.140745

Pey, J., Querol, X., Alastuey, A., Forastiere, F., & Stafoggia, M. (2013). African dust outbreaks over the Mediterranean Basin during 2001–2011: PM10 concentrations, phenomenology and trends, and its relation with synoptic and mesoscale meteorology. *Atmospheric Chemistry and Physics*, *13*(3), 1395–1410. https://doi.org/10.5194/acp-13-1395-2013

Prospero, J. M., Ginoux, P., Torres, O., Nicholson, S. E., & Gill, T. E. (2002). Environmental characterization of global sources of atmospheric soil dust identified with the Nimbus 7 Total Ozone Mapping Spectrometer (TOMS) absorbing aerosol product. *Reviews of Geophysics*, *40*(1). https://doi.org/10.1029/2000rg000095

Remias, D., Karsten, U., Lütz, C., & Leya, T. (2010). Physiological and morphological processes in the Alpine snow alga Chloromonas nivalis (Chlorophyceae) during cyst formation. *Protoplasma*, *243*(1–4), 73–86. https://doi.org/10.1007/s00709-010-0123-y

Réveillet, M., Dumont, M., Gascoin, S., Lafaysse, M., Nabat, P., Ribes, A., Nheili, R., Tuzet, F., Ménégoz, M., Morin, S., Picard, G., & Ginoux, P. (2022). Black carbon and dust alter the response of mountain snow cover under climate change. *Nature Communications*, *13*(1). https://doi.org/10.1038/s41467-022-32501-y

Réveillet, M., Dumont, M., Gascoin, S., Nabat, P., Lafaysse, M., Nheili, R., Tuzet, F., Menegoz, M., & Ginoux, P. (2020). *Role of Saharan dust and black carbon*

https://doi.org/10.5194/egusphere-2026-4306
Preprint. Discussion started: 21 August 2026

deposition on snow cover in the French mountain ranges over the last 39 years. Copernicus GmbH. https://doi.org/10.5194/egusphere-egu2020-15209

Revuelto, J., Azorin-Molina, C., Alonso-González, E., Sanmiguel-Vallelado, A., Navarro-Serrano, F., Rico, I., & López-Moreno, J. I. (2017). Meteorological and snow distribution data in the Izas Experimental Catchment (Spanish Pyrenees) from 2011 to 2017. *Earth System Science Data*, *9*(2), 993–1005. https://doi.org/10.5194/essd-9-993-2017

Revuelto, J., Gómez, D., Alonso-González, E., Vidaller, I., Rojas-Heredia, F., Deschamps-Berger, C., García-Jiménez, J., Rodríguez-López, G., Sobrino, J., Montorio, R., Perez-Cabello, F., & López-Moreno, J. I. (2022). Intermediate snowpack melt-out dates guarantee the highest seasonal grasslands greening in the Pyrenees. *Scientific Reports*, *12*(1). https://doi.org/10.1038/s41598-022-22391-x

Reynolds, R. L., Goldstein, H. L., Moskowitz, B. M., Bryant, A. C., Skiles, S. M., Kokaly, R. F., Flagg, C. B., Yauk, K., Berquó, T., Breit, G., Ketterer, M., Fernandez, D., Miller, M. E., & Painter, T. H. (2014). Composition of dust deposited to snow cover in the Wasatch Range (Utah, USA): Controls on radiative properties of snow cover and comparison to some dust-source sediments. *Aeolian Research*, *15*, 73–90. https://doi.org/10.1016/j.aeolia.2013.08.001

Rostási, Á., Topa, B. A., Gresina, F., Weiszburg, T. G., Gelencsér, A., & Varga, G. (2022). Saharan dust deposition in central europe in 2016—A representative year of the increased north african dust removal over the last decade. *Frontiers in Earth Science*, *10*. https://doi.org/10.3389/feart.2022.869902

Salvador, P., Pey, J., Pérez, N., Alastuey, A., Querol, X., & Artíñano, B. (2024). Estimating the probability of occurrence of African dust outbreaks over regions of the western Mediterranean basin from thermodynamic atmospheric parameters. *Science of the Total Environment*, *922*, 171307. https://doi.org/10.1016/j.scitotenv.2024.171307

Salvador, P., Pey, J., Pérez, N., Querol, X., & Artíñano, B. (2022). Increasing atmospheric dust transport towards the western Mediterranean over 1948–2020. *Npj Climate and Atmospheric Science*, *5*(1). https://doi.org/10.1038/s41612-022-00256-4

Schmale, J., Zieger, P., & Ekman, A. M. L. (2021). Aerosols in current and future Arctic climate. *Nature Climate Change*, *11*(2), 95–105. https://doi.org/10.1038/s41558-020-00969-5

https://doi.org/10.5194/egusphere-2026-4306
Preprint. Discussion started: 21 August 2026

Shao, Y., Wyrwoll, K.-H., Chappell, A., Huang, J., Lin, Z., McTainsh, G. H., Mikami, M., Tanaka, T. Y., Wang, X., & Yoon, S. (2011). Dust cycle: An emerging core theme in Earth system science. *Aeolian Research*, *2*(4), 181–204. https://doi.org/10.1016/j.aeolia.2011.02.001

Skiles, S. M., Flanner, M., Cook, J. M., Dumont, M., & Painter, T. H. (2018). Radiative forcing by light-absorbing particles in snow. *Nature Climate Change*, *8*(11), 964–971. https://doi.org/10.1038/s41558-018-0296-5

Skiles, S. M, & Painter, T. H. (2018). Assessment of radiative forcing by light-absorbing particles in snow from in situ observations with radiative transfer modeling. *Journal of Hydrometeorology*, *19*(8), 1397–1409. https://doi.org/10.1175/jhm-d-18-0072.1

Skiles, S. M., & Painter, T. H. (2019). Toward understanding direct absorption and grain size feedbacks by dust radiative forcing in snow with coupled snow physical and radiative transfer modeling. *Water Resources Research*, *55*(8), 7362–7378. https://doi.org/10.1029/2018wr024573

Skiles, S. M., Painter, T. H., Deems, J. S., Bryant, A. C., & Landry, C. C. (2012). Dust radiative forcing in snow of the Upper Colorado River Basin: 2. Interannual variability in radiative forcing and snowmelt rates. *Water Resources Research*, *48*(7). https://doi.org/10.1029/2012wr011986

Sproles, E. A., Mullen, A., Hendrikx, J., Gatebe, C., & Taylor, S. (2020). Autonomous aerial vehicles (aavs) as a tool for improving the spatial resolution of snow albedo measurements in mountainous regions. *Hydrology*, *7*(3), 41. https://doi.org/10.3390/hydrology7030041

Sterle, K. M., McConnell, J. R., Dozier, J., Edwards, R., & Flanner, M. G. (2013). Retention and radiative forcing of black carbon in eastern Sierra Nevada snow. *The Cryosphere*, *7*(1), 365–374. https://doi.org/10.5194/tc-7-365-2013

Sun, J., Birmili, W., Hermann, M., Tuch, T., Weinhold, K., Merkel, M., Rasch, F., Müller, T., Schladitz, A., Bastian, S., Löschau, G., Cyrys, J., Gu, J., Flentje, H., Briel, B., Asbach, C., Kaminski, H., Ries, L., Sohmer, R., … Wiedensohler, A. (2020). Decreasing trends of particle number and black carbon mass concentrations at 16 observational sites in Germany from 2009 to 2018. *Atmospheric Chemistry and Physics*, *20*(11), 7049–7068. https://doi.org/10.5194/acp-20-7049-2020

https://doi.org/10.5194/egusphere-2026-4306
Preprint. Discussion started: 21 August 2026

Switanek, M., Resch, G., Gobiet, A., Günther, D., Marty, C., & Schöner, W. (2024). Snow depth sensitivity to mean temperature, precipitation, and elevation in the Austrian and Swiss Alps. *The Cryosphere*, *18*(12), 6005–6026. https://doi.org/10.5194/tc-18-6005-2024

The IPCC 2007 report. (2007). *Climate Change*, 480–481. https://doi.org/10.1017/cbo9780511803826.013

Tinorua, S., Denjean, C., Nabat, P., Bourrianne, T., Pont, V., Gheusi, F., & Leclerc, E. (2024). Higher absorption enhancement of black carbon in summer shown by 2-year measurements at the high-altitude mountain site of Pic du Midi Observatory in the French Pyrenees. *Atmospheric Chemistry and Physics*, *24*(3), 1801–1824. https://doi.org/10.5194/acp-24-1801-2024

Tuzet, F., Dumont, M., Lafaysse, M., Picard, G., Arnaud, L., Voisin, D., Lejeune, Y., Charrois, L., Nabat, P., & Morin, S. (2017). A multilayer physically based snowpack model simulating direct and indirect radiative impacts of light-absorbing impurities in snow. *The Cryosphere*, *11*(6), 2633–2653. https://doi.org/10.5194/tc-11-2633-2017

Tuzet, F., Dumont, M., Picard, G., Lamare, M., Voisin, D., Nabat, P., Lafaysse, M., Larue, F., Revuelto, J., & Arnaud, L. (2020). Quantification of the radiative impact of light-absorbing particles during two contrasted snow seasons at Col du Lautaret (2058 m a.s.l., French Alps). *The Cryosphere*, *14*(12), 4553–4579. https://doi.org/10.5194/tc-14-4553-2020

Valt, M., & Cianfarra, P. (2010). Recent snow cover variability in the Italian Alps. *Cold Regions Science and Technology*, *64*(2), 146–157. https://doi.org/10.1016/j.coldregions.2010.08.008

Varga, G., Cserháti, C., Kovács, J., Szeberényi, J., & Bradák, B. (2014). Unusual Saharan dust events in the Carpathian Basin (Central Europe) in 2013 and early 2014. *Weather*, *69*(11), 309–313. https://doi.org/10.1002/wea.2334

Vaughan, D. G., Comiso, J. C., Allison, I., Carrasco, J., Kaser, G., Kwok, R., Mote, P., Murray, T., Paul, F., Ren, J., Rignot, E., Solomina, O., Steffen, K., & Zhang, T. (2013). Observations: Cryosphere. In T. F. Stocker, D. Qin, G.-K. Plattner, M. M. B. Tignor, S. K. Allen, J. Boschung, A. Nauels, Y. Xia, V. Bex, & P. M. Midgley (Eds.), *Climate change 2013: The physical science basis. Contribution of Working*

Group I to the Fifth Assessment Report of the Intergovernmental Panel on Climate Change (pp. 317–382). Cambridge University Press.

Wittmann, M., Groot Zwaaftink, C. D., Steffensen Schmidt, L., Guðmundsson, S., Pálsson, F., Arnalds, O., Björnsson, H., Thorsteinsson, T., & Stohl, A. (2017). Impact of dust deposition on the albedo of Vatnajökull ice cap, Iceland. *The Cryosphere*, *11*(2), 741–754. https://doi.org/10.5194/tc-11-741-2017